Appendix A
Results of Triaxial and Consolidation Tests

Triaxial and consolidation tests were performed on specimens of the soils used for interface testing. The objectives of these tests were as follows:

a. Determination of the internal friction angle of the soils.

b. Determination of the hyperbolic parameters of the soils.

c. Evaluation of hydrocompression strains induced by inundation of the soils.

This appendix describes the procedures and results of the tests performed on specimens of Density Sand and Light Castle Sand. The procedure for the determination of the internal friction angle of the soils from the results of the triaxial tests is presented. Hydrocompression properties of the soils are evaluated based on the results of the consolidation tests. The procedure for determination of the hyperbolic parameter values of each of the soils is presented in Appendix B.

A.1 Triaxial Tests

Two different sands were used for the tests:

a. Density Sand. It is a fine-to-medium silica sand with subrounded to rounded grains, available commercially for in situ density determinations.

b. Light Castle Sand. It is a fine-to-medium sand with subangular to angular grains.

A more complete description of the properties of these soils is presented in Chapter 3 of this Dissertation.

Drained triaxial (CD) tests were performed to determine the internal friction angle and hyperbolic parameter values of the Density Sand and the Light Castle Sand for a range of relative densities. Sets of medium dense and dense specimens were prepared by pluviation for each type of sand. After preparation, each sample was subjected to an internal manometric pressure of -15 to -20 kPa, which was gradually removed during application of the cell pressure. The samples were de-aired using CO_2, inundated with de-aired distilled water, and backpressure saturated. The samples in each set were consolidated under effective confining pressures ranging from 45 to 280 kPa. These values are representative of the estimated values of confining pressure within the backfill of typical lock walls. Shearing was performed at a strain rate of 0.25 $^{\%}/_{\min}$, which was found to be appropriate for pore pressure dissipation during previous trials.

The results of the tests are presented graphically in Figures A1 to A4[1]. All the specimens exhibited dilation during shear and strain softening after mobilization of the peak strength. Because the peak strength envelopes of both soils are curved, the value of secant friction angle ϕ for a given confining pressure σ'_3 can be calculated from the following expression (Duncan et al., 1980)[2]:

$$\phi = \phi_o - \Delta\phi \cdot \log_{10}\left(\frac{\sigma'_3}{p_a}\right) \qquad \text{(A1)}$$

where

ϕ_o = peak secant friction at a confining pressure of 101.4 kPa (1 atm)

$\Delta\phi$ = reduction in the peak friction angle value for a tenfold increase in σ'_3

p_a = atmospheric pressure (101.3 kPa)

The values of friction parameters ϕ_o and $\Delta\phi$ are determined using diagrams of secant friction angle versus normalized confining pressure σ'_3/p_a such as those shown in Figures A1c, A2c, A3c, and A4c.

The procedure for the determination of the hyperbolic parameter values of the soils is presented in Appendix B.

---

[1] For convenience, symbols are listed and defined in the Notation (Appendix F)

[2] References cited in this Appendix are included in the References at the end of the main text

A.2 Consolidation Testing

Consolidation tests were performed on specimens of Density Sand and Light Castle Sand to provide additional data on their mechanical properties and determine their susceptibility to hydrocompression (Brandon, Duncan, and Gardner 1990).

Two specimens of each type of sand were prepared at different relative densities in a dry condition. Each specimen was consolidated under a series of vertical stress increments. Once a predetermined stress was reached, the specimen was inundated after primary consolidation was attained. The results of these tests are presented as strain versus stress diagrams in Figures A5 to A8.

During inundation, compressive vertical strain was observed in all specimens tested. The strain that takes place during inundation includes deformation due to secondary compression of the sand and collapse of the structure due to inundation. The value of the strain induced by hydrocompression in each test was determined from strain versus time plots following the procedure suggested by Brandon, Duncan, and Gardner (1990).

Figure A9 is a diagram of hydrocompression strain versus relative density determined from the consolidation tests on Light Castle Sand specimens. Two specimens, prepared at different relative densities, were inundated under a vertical stress of 32.3 kPa. It is seen that hydrocompression strains decrease for increasing soil densities. A straight line was drawn through the data points corresponding to these two tests and extended through the entire range of relative densities shown. Lines parallel to this extended line were drawn through the single data points corresponding to vertical stresses of 7.8 and 17 kPa.

In the Instrumented Retaining Wall (IRW) described in Chapter 5, the vertical stress in the backfill ranges from zero at the top of the backfill to 33.6 kPa at the bottom. The extended lines shown in Figure A9 allow the estimation of hydrocompression strains throughout the height of the backfill. It can be seen that hydrocompression strains may range from zero to 0.0015 for a relative density of 100 percent. Assuming an average vertical stress of 17 kPa, the average hydrocompression strain of the backfill during inundation is 0.0002. This value corresponds to a vertical settlement at the top of the backfill of less than 0.5 mm. This is consistent with the negligible settlements observed during inundation in the IRW test.

It must be noted that the procedure followed for estimation of hydrocompression strains in the IRW backfill is only approximate. There is not enough information to support the assumed linear relationship between hydrocompression strains and relative density. In addition, an accurate estimate of the backfill settlement can be obtained only by integration of the hydrocompression strains over the height of the backfill. However, given the relatively small height of the IRW backfill, it can be assumed that the error in the estimation of the hydrocompression settlement is small.

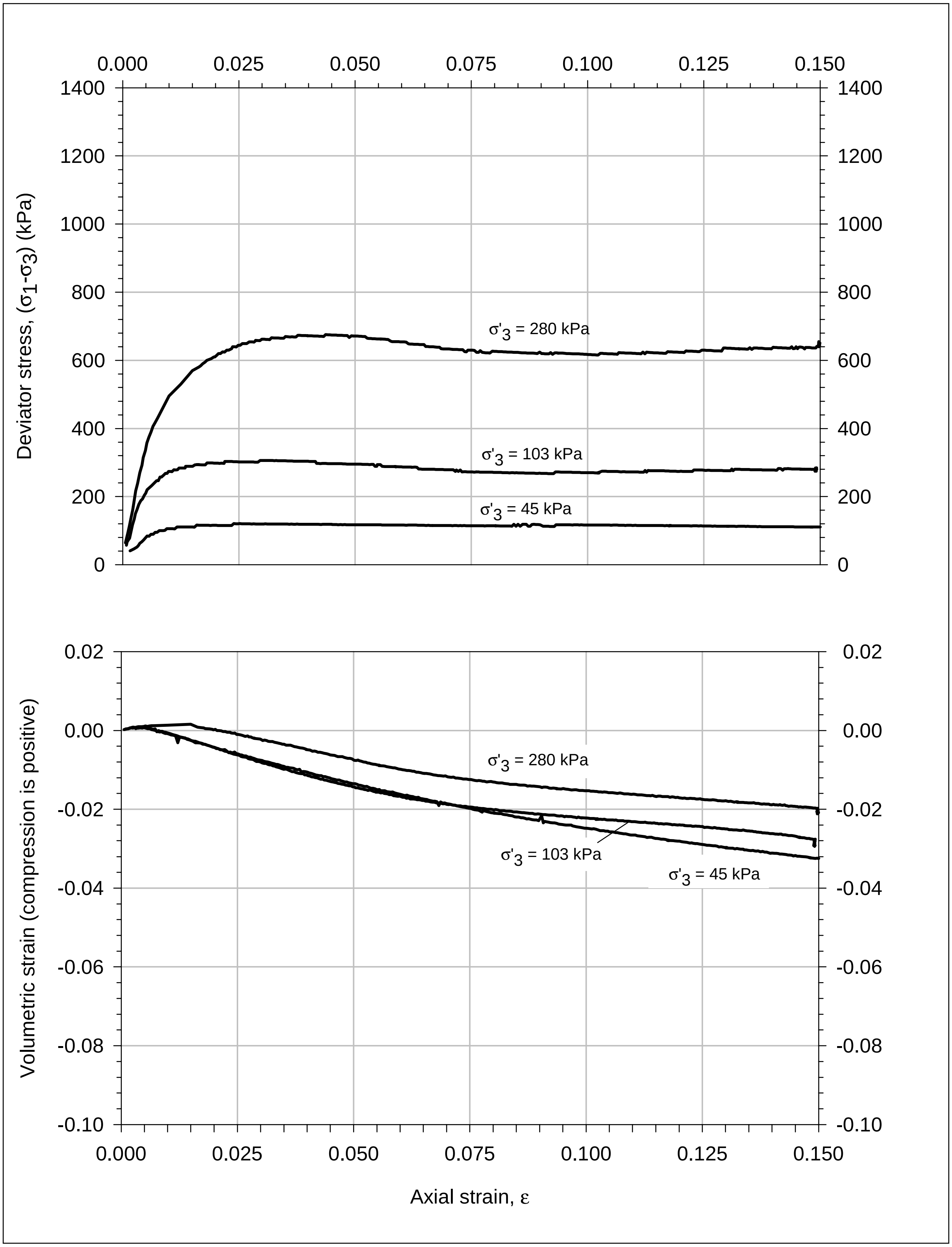

a) Stress-strain and volumetric strain data

Figure A1. Results of CD triaxial tests on medium dense Density Sand (Sheet 1 of 3)

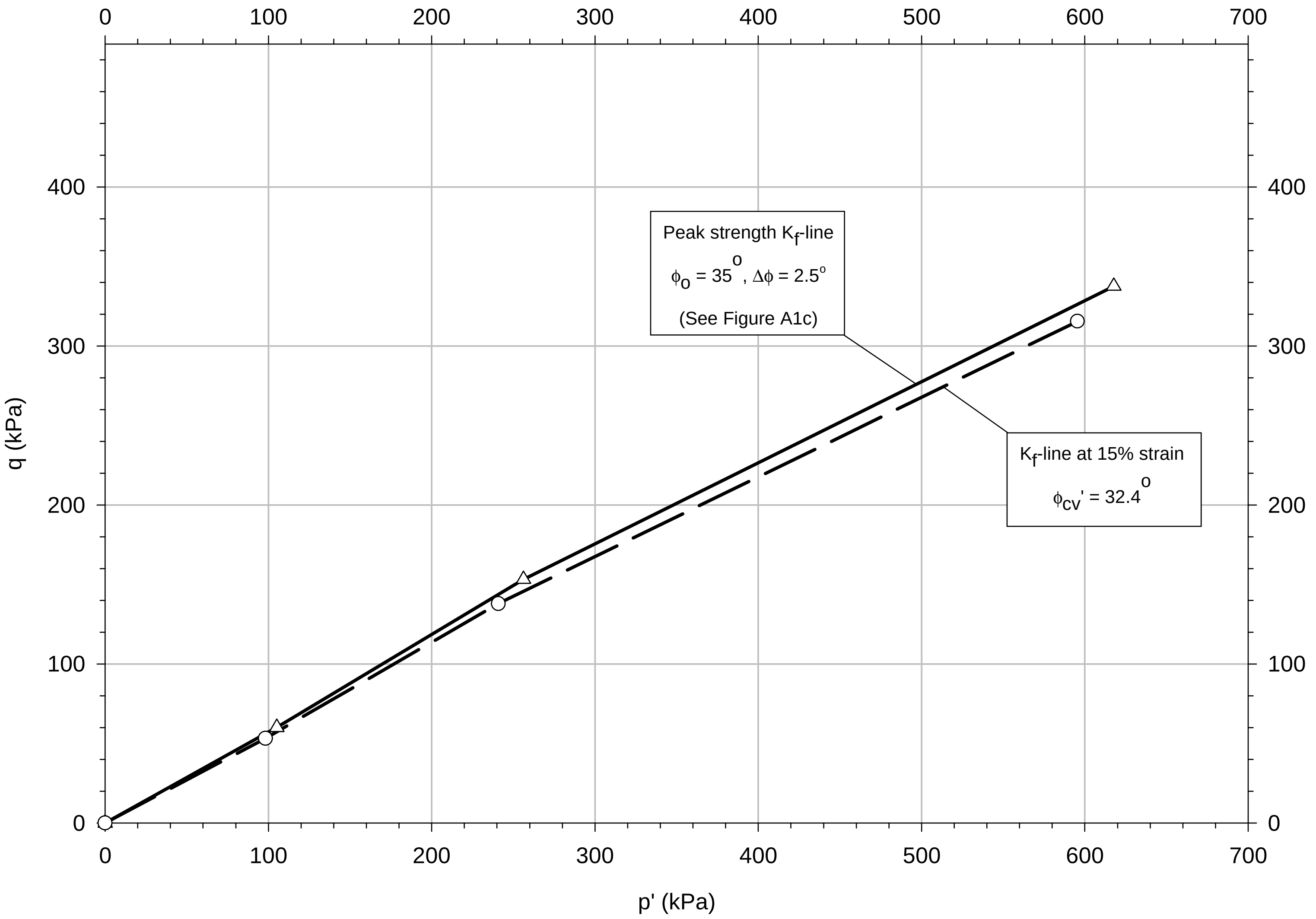

b) Peak strength and 15-percent strain K_f-lines

Figure A1. (Sheet 2 of 3)

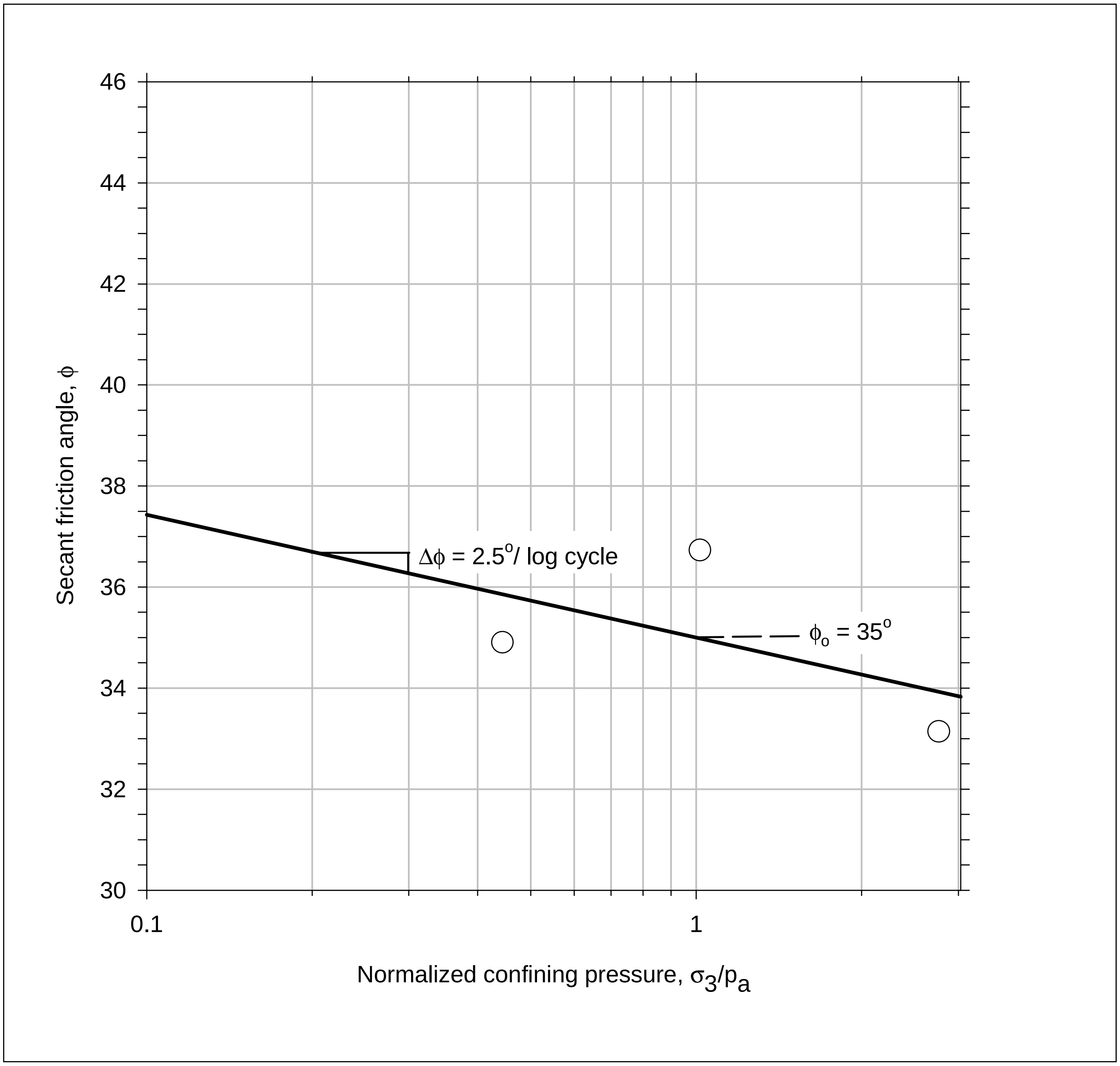

c) Determination of strength parameters ϕ_o and $\Delta\phi$

Figure A1. (Sheet 3 of 3)

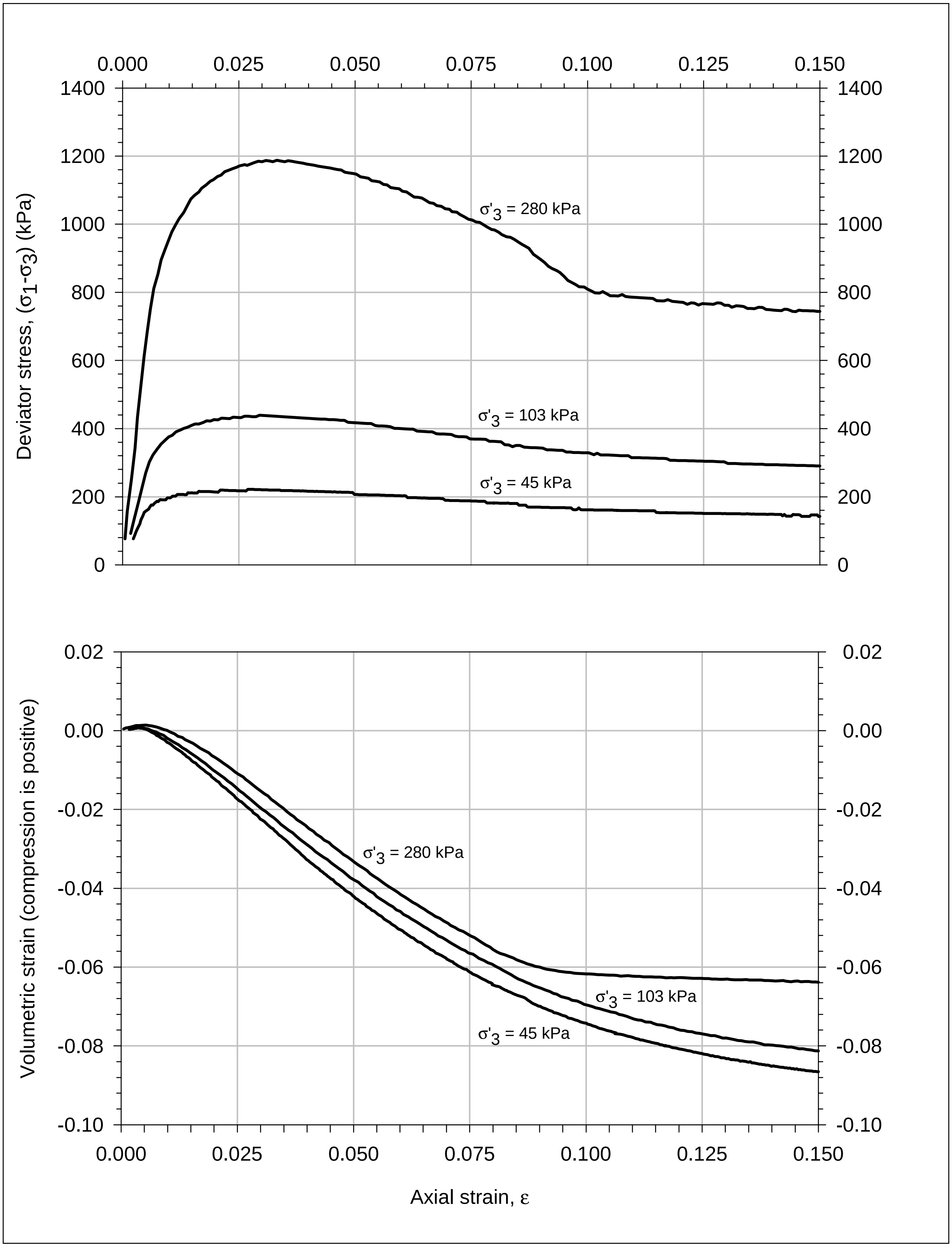

a) Stress-strain and volumetric strain data

Figure A2. Results of CD triaxial tests on dense Density Sand (Sheet 1 of 3)

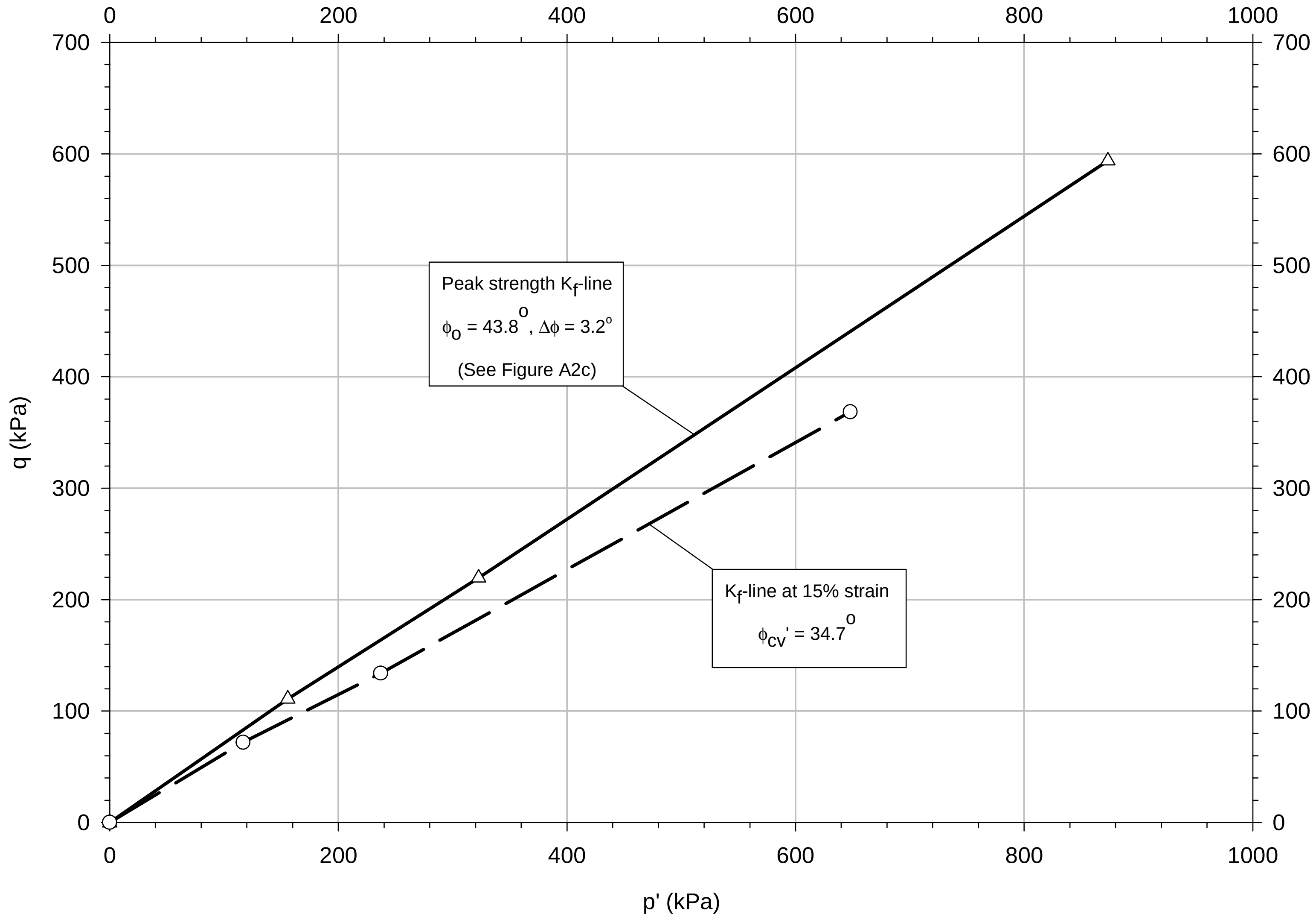

b) Peak strength and 15-percent strain K$_f$-lines

Figure A2. (Sheet 2 of 3)

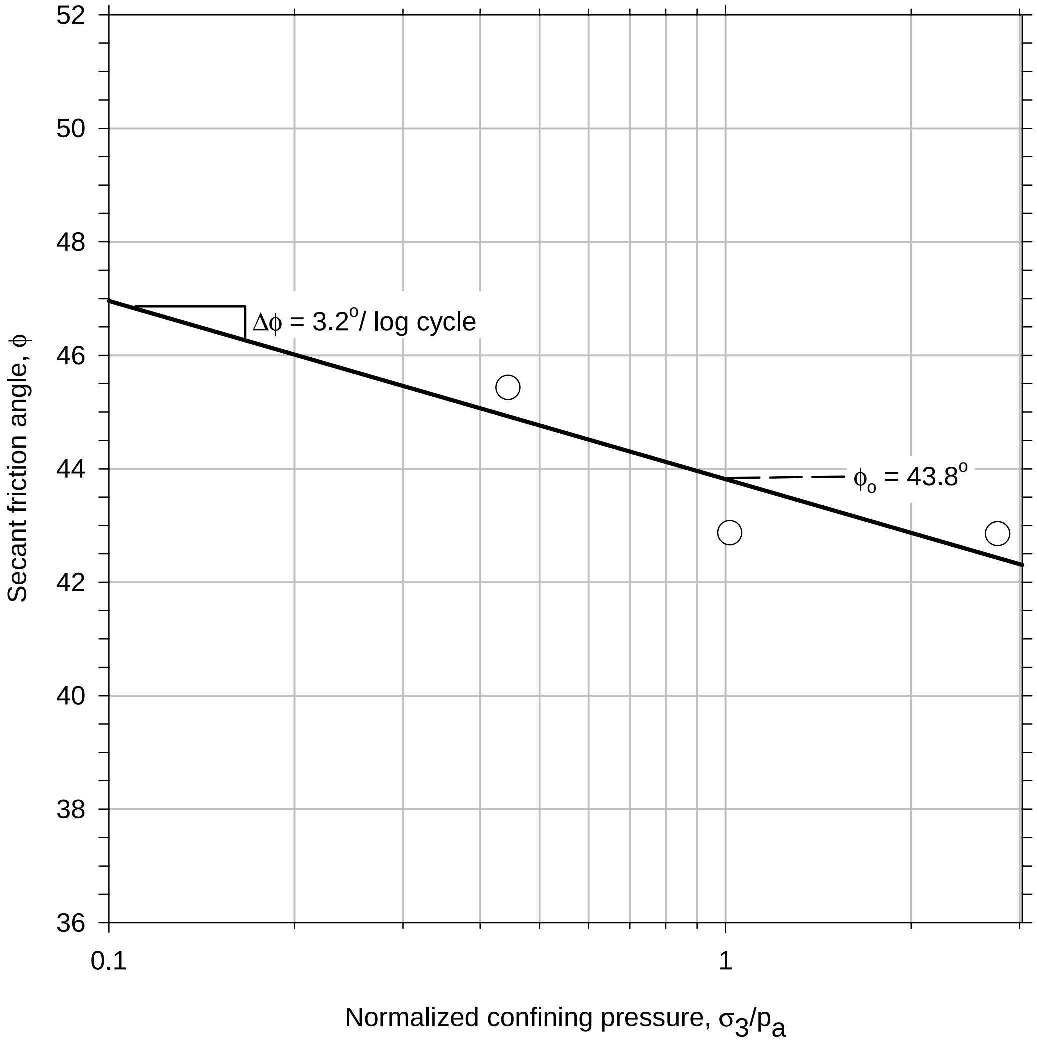

c) Determination of strength parameters ϕ_o and $\Delta\phi$

Figure A2. (Sheet 3 of 3)

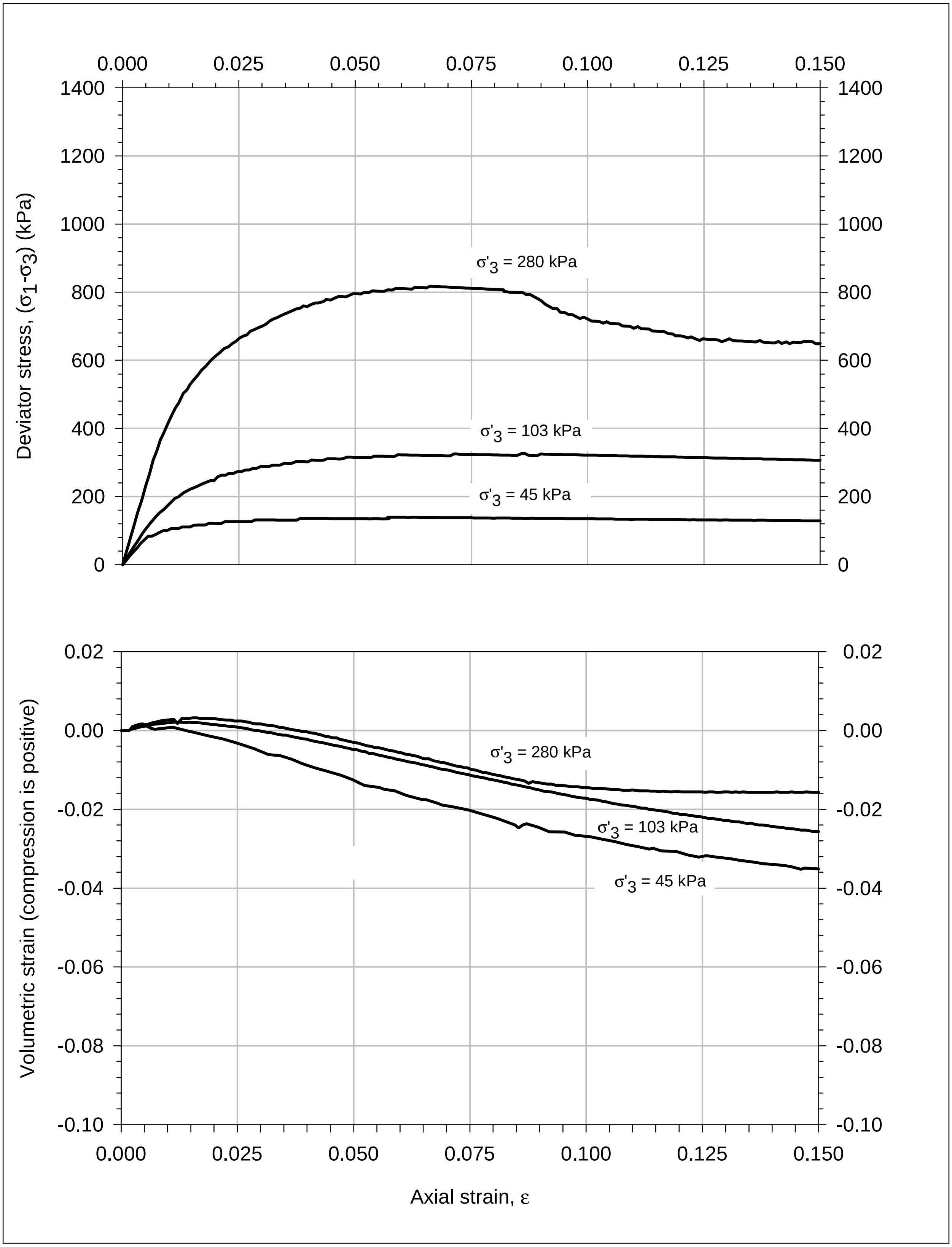

a) Stress-strain and volumetric strain data

Figure A3. Results of CD triaxial tests on medium dense Light Castle Sand (Sheet 1 of 3)

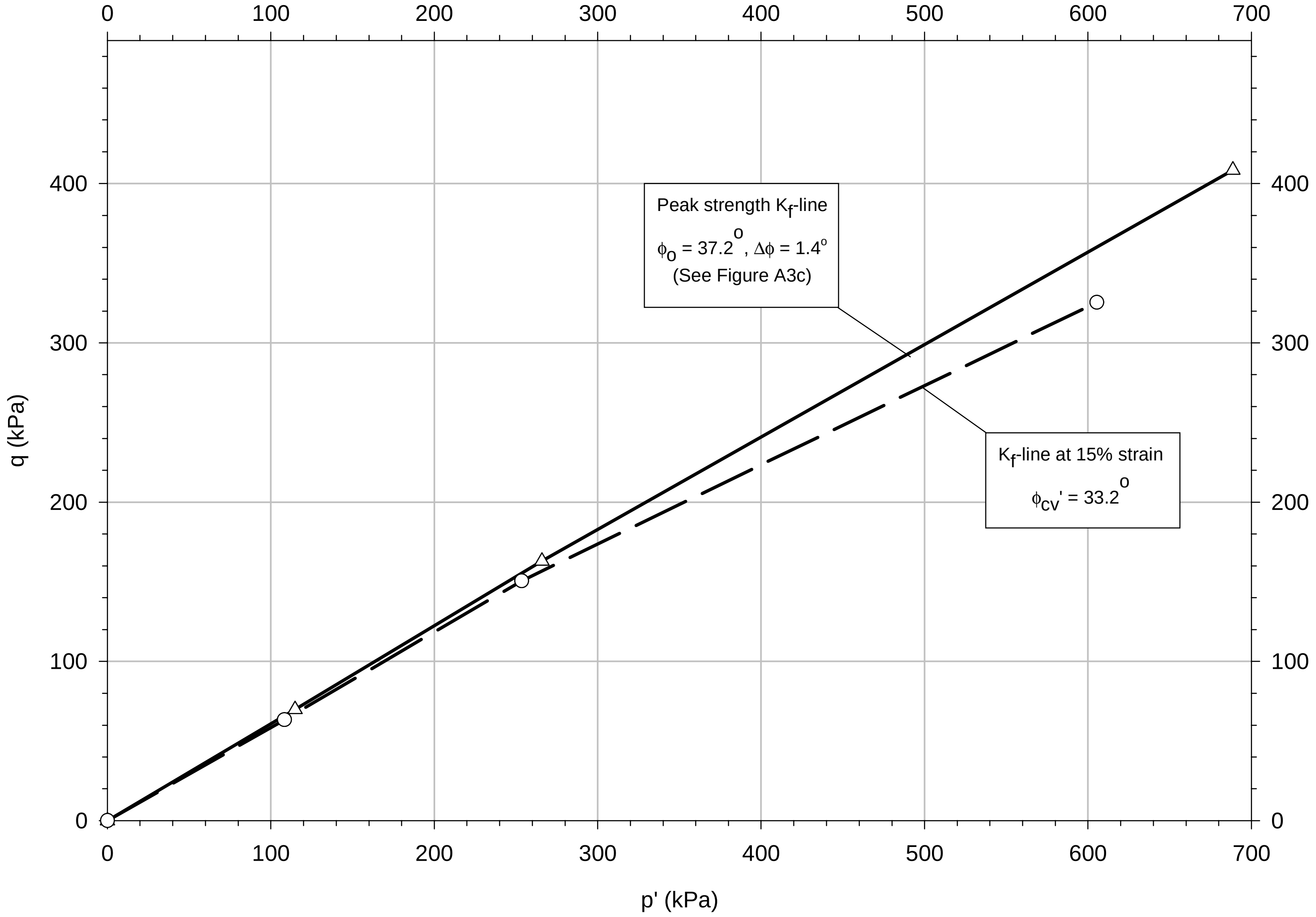

b) Peak strength and 15-percent strain K_f-lines

Figure A3. (Sheet 2 of 3)

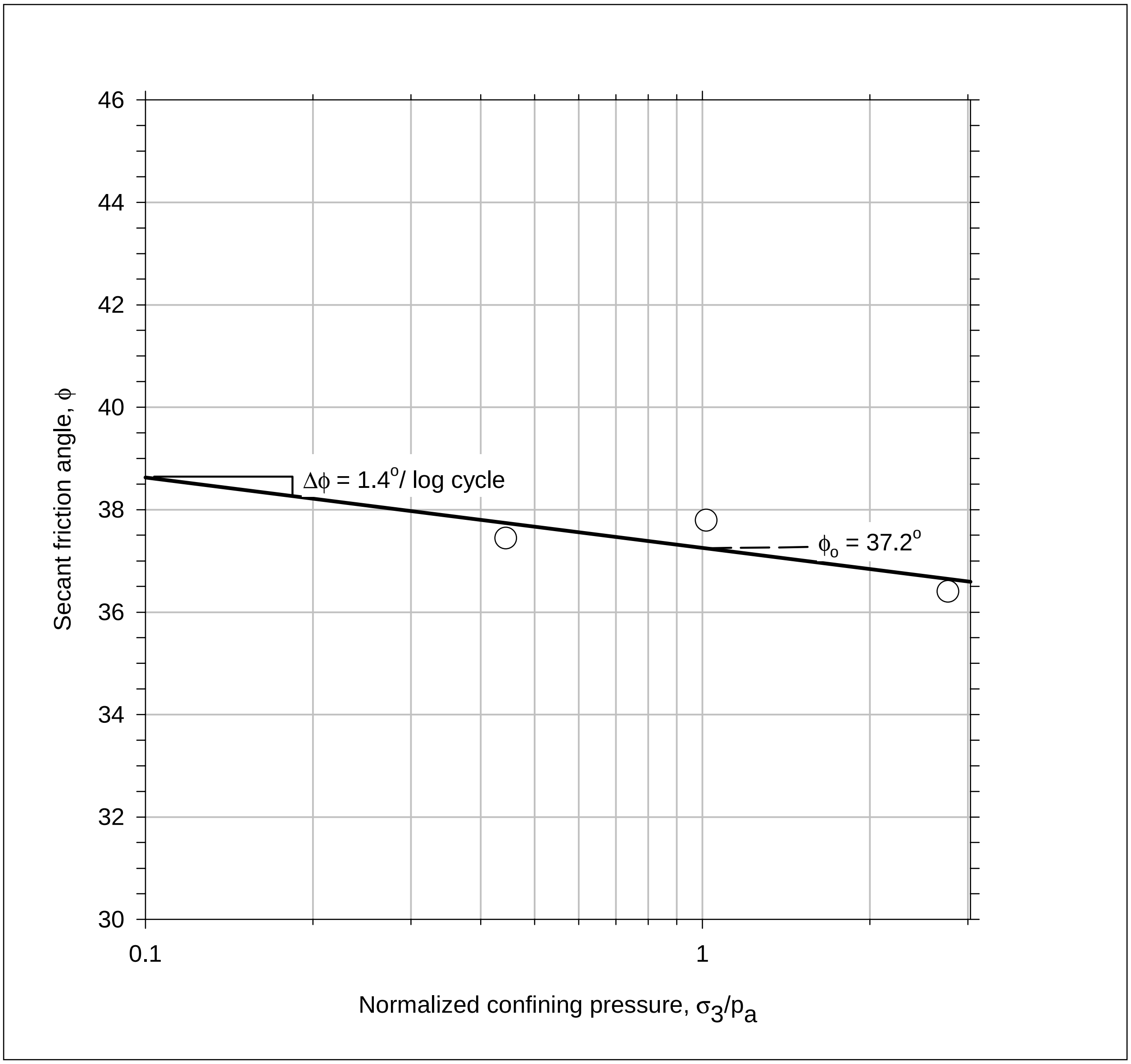

c) Determination of strength parameters ϕ_o and $\Delta\phi$

Figure A3. (Sheet 3 of 3)

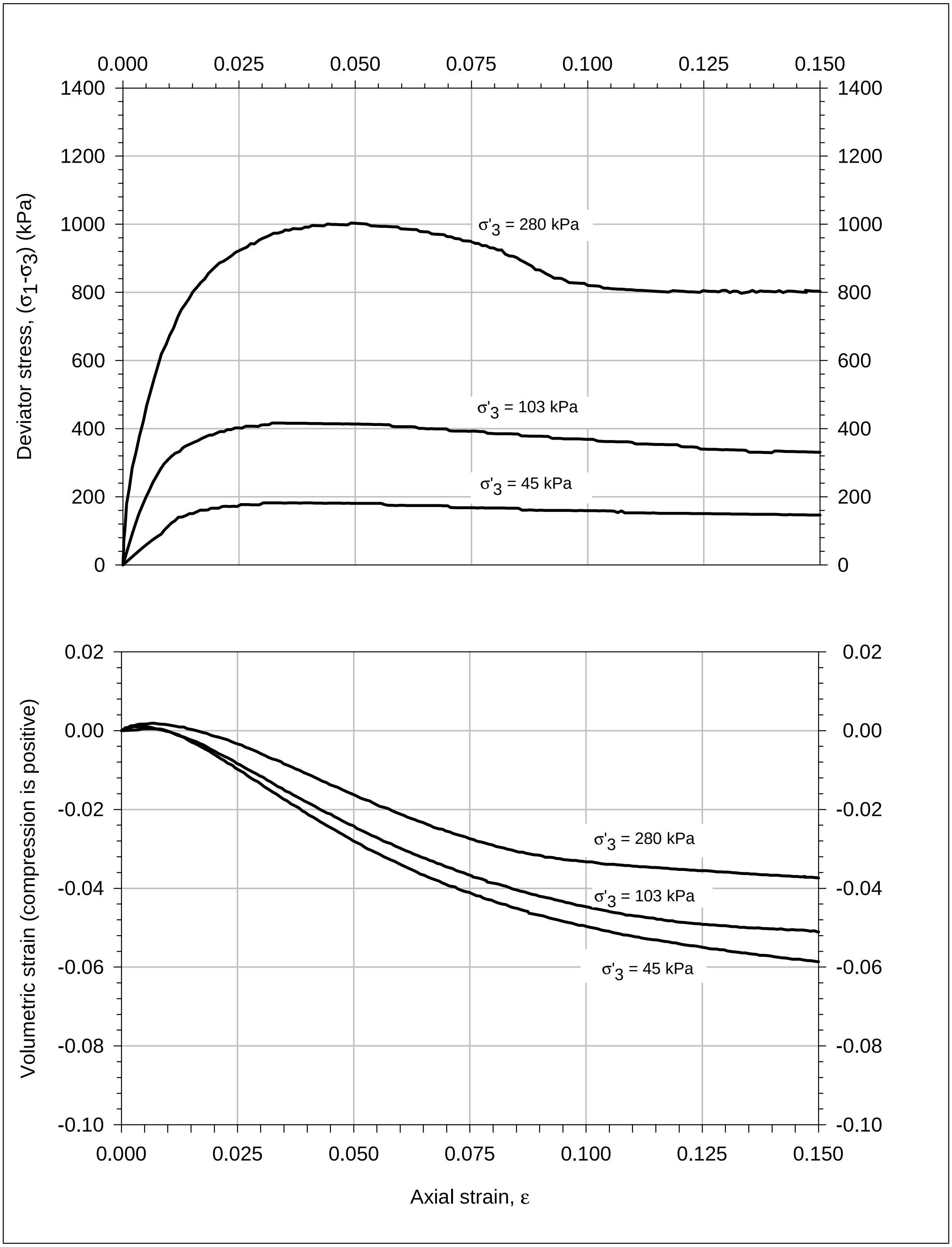

a) Stress-strain and volumetric strain data

Figure A4. Results of CD triaxial tests on dense Light Castle Sand (Sheet 1 of 3)

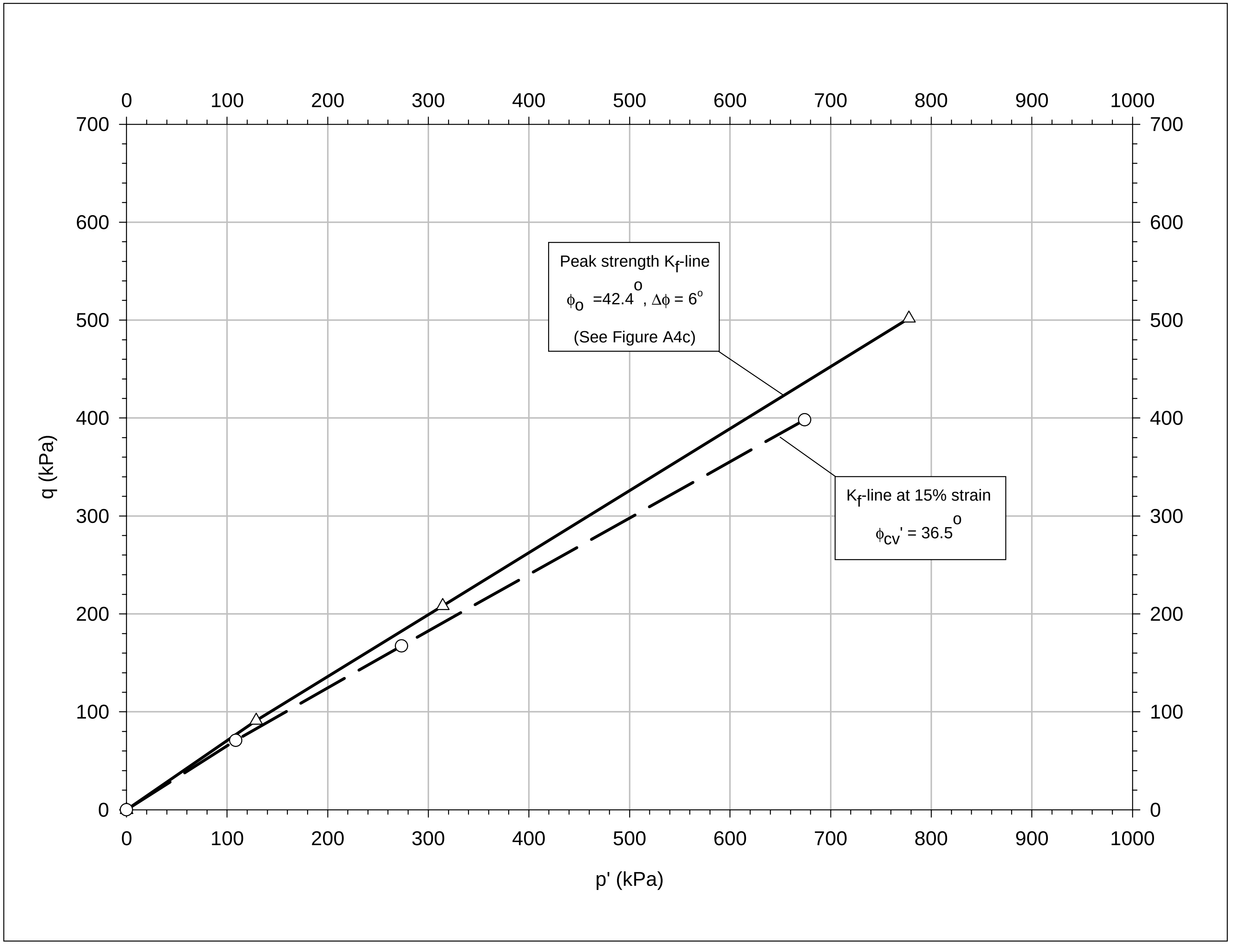

b) Peak strength and 15-percent strain K_f-lines

Figure A4. (Sheet 2 of 3)

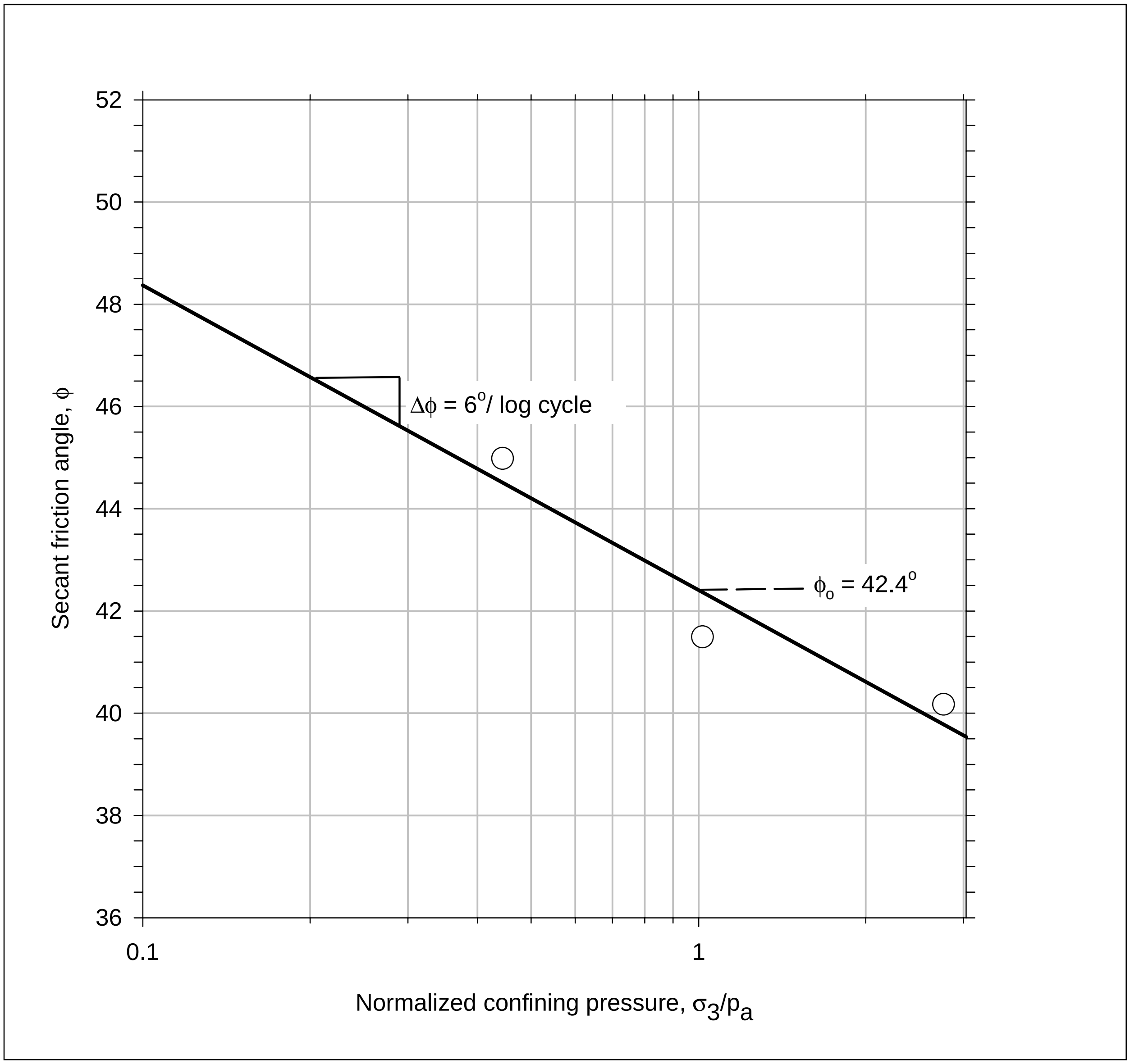

c) Determination of strength parameters ϕ_o and $\Delta\phi$

Figure A4. (Sheet 3 of 3)

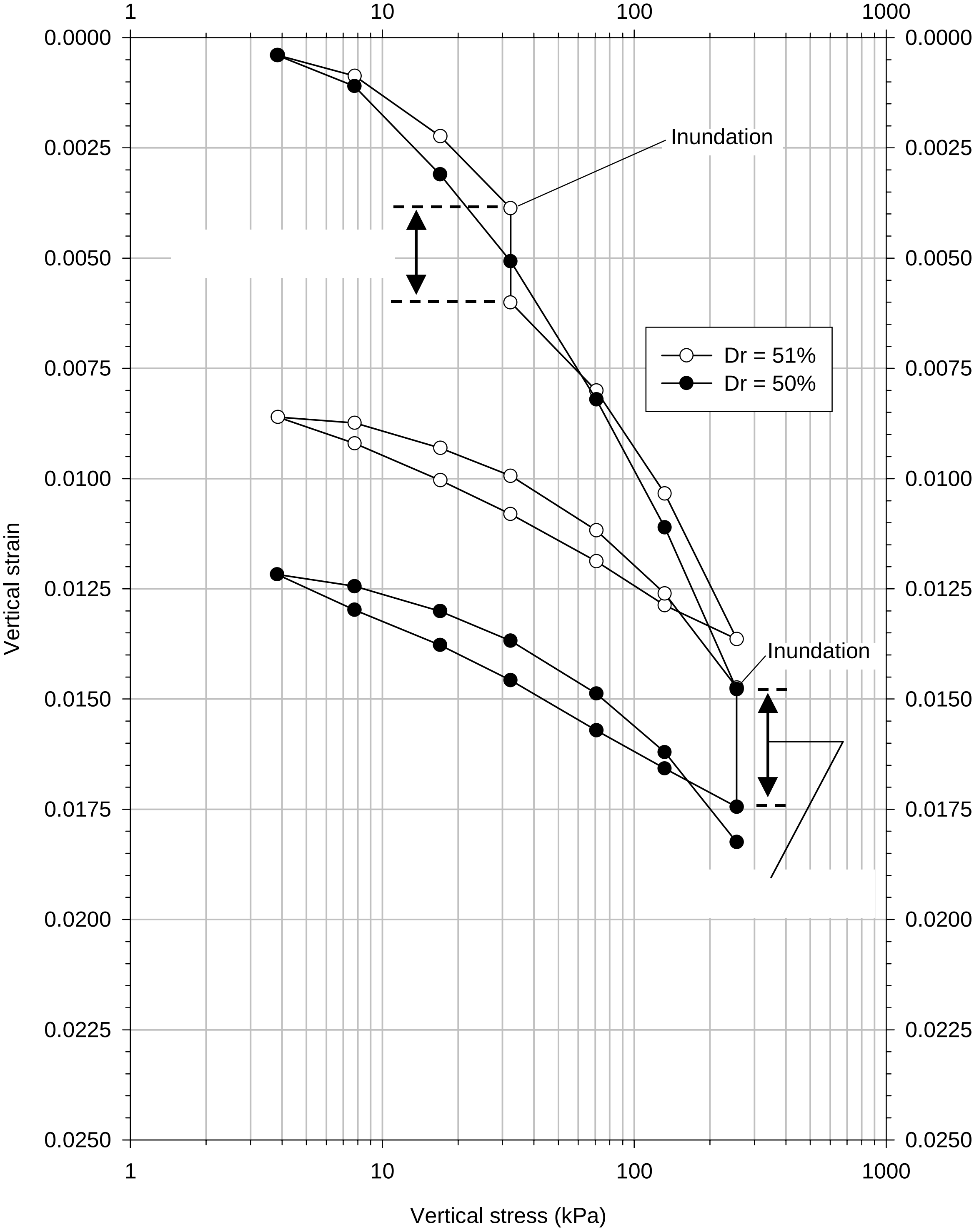

Figure A5. Results of consolidation tests on medium dense Density Sand

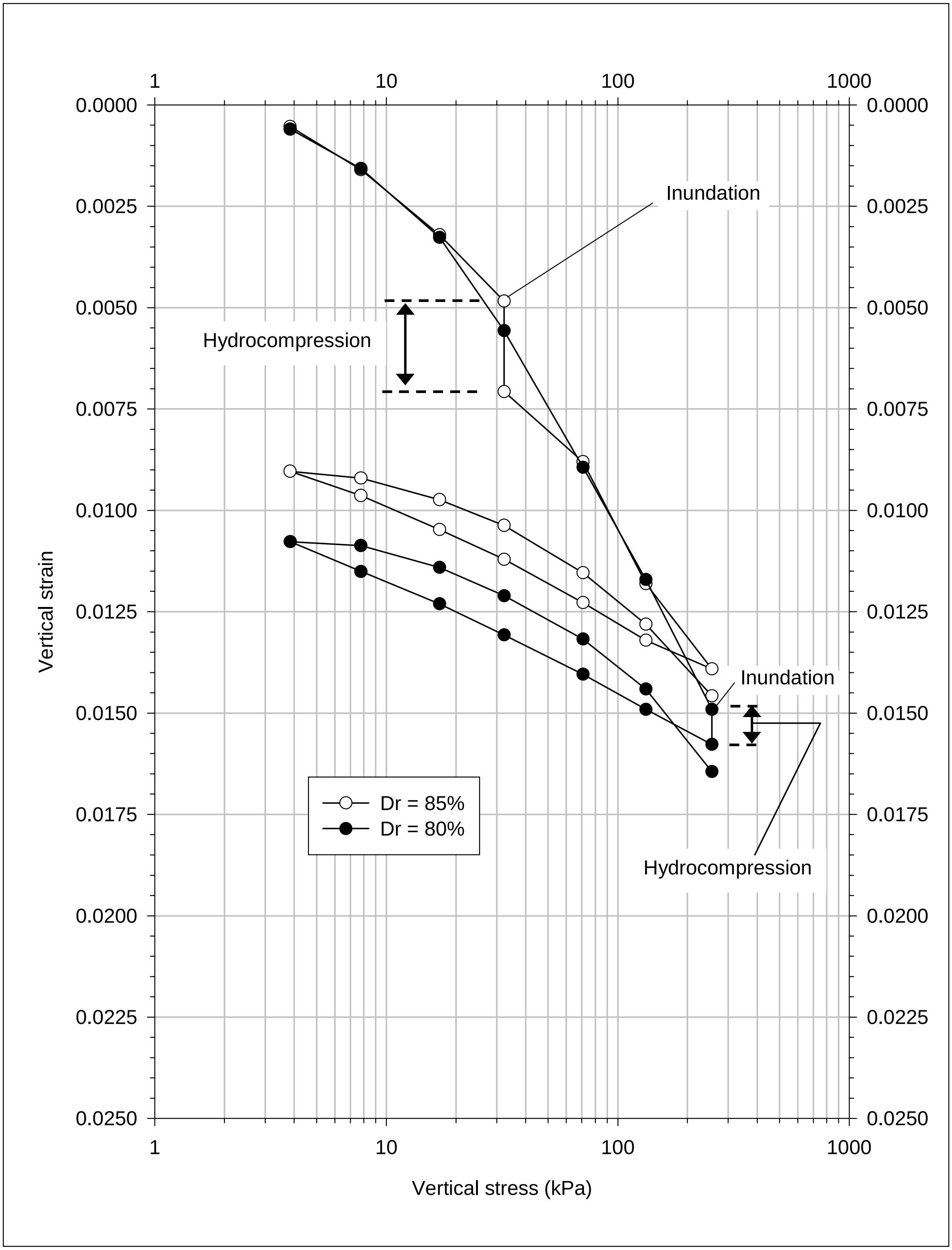

Figure A6. Results of consolidation tests on dense Density Sand

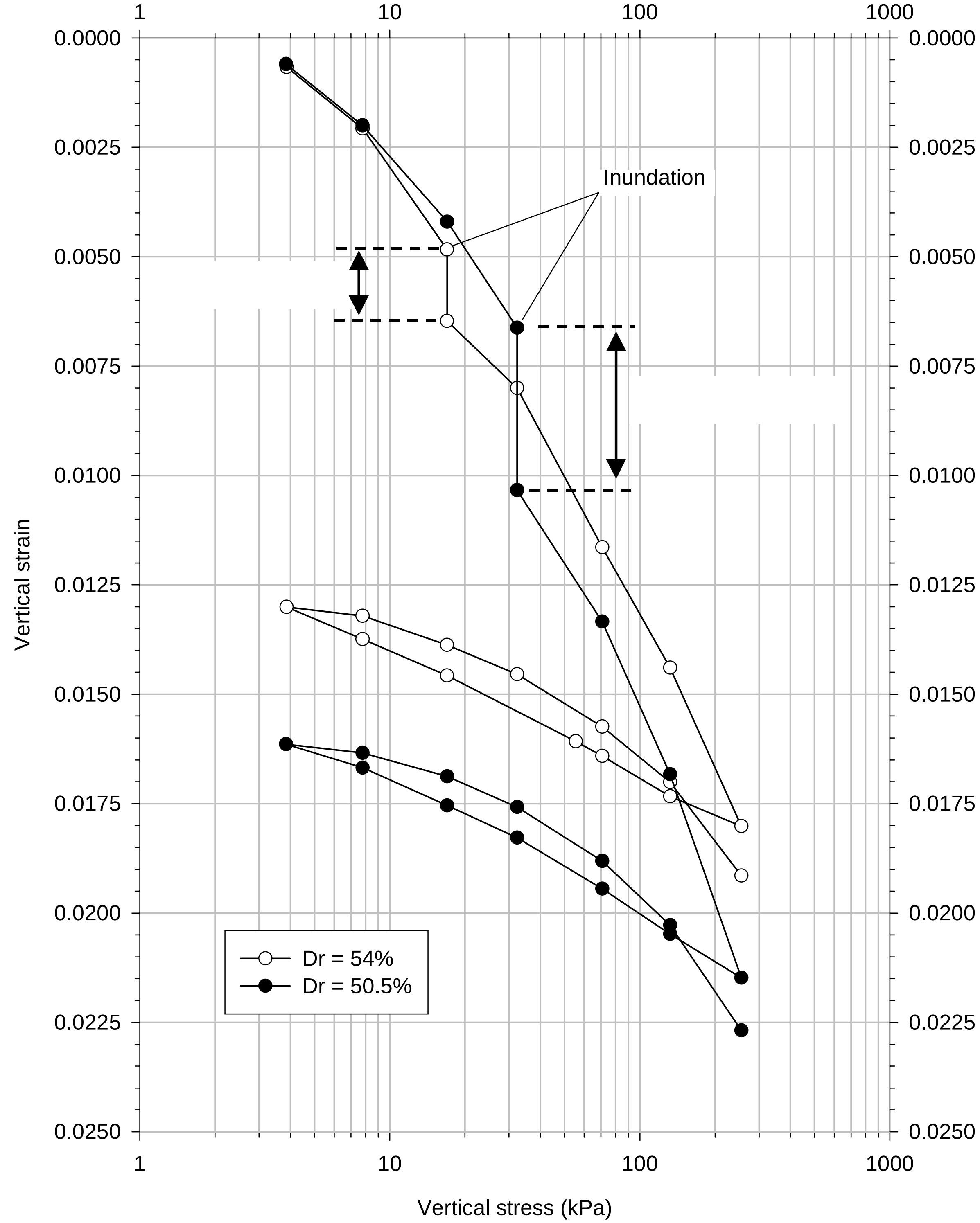

Figure A7. Results of consolidation tests on medium dense Light Castle Sand

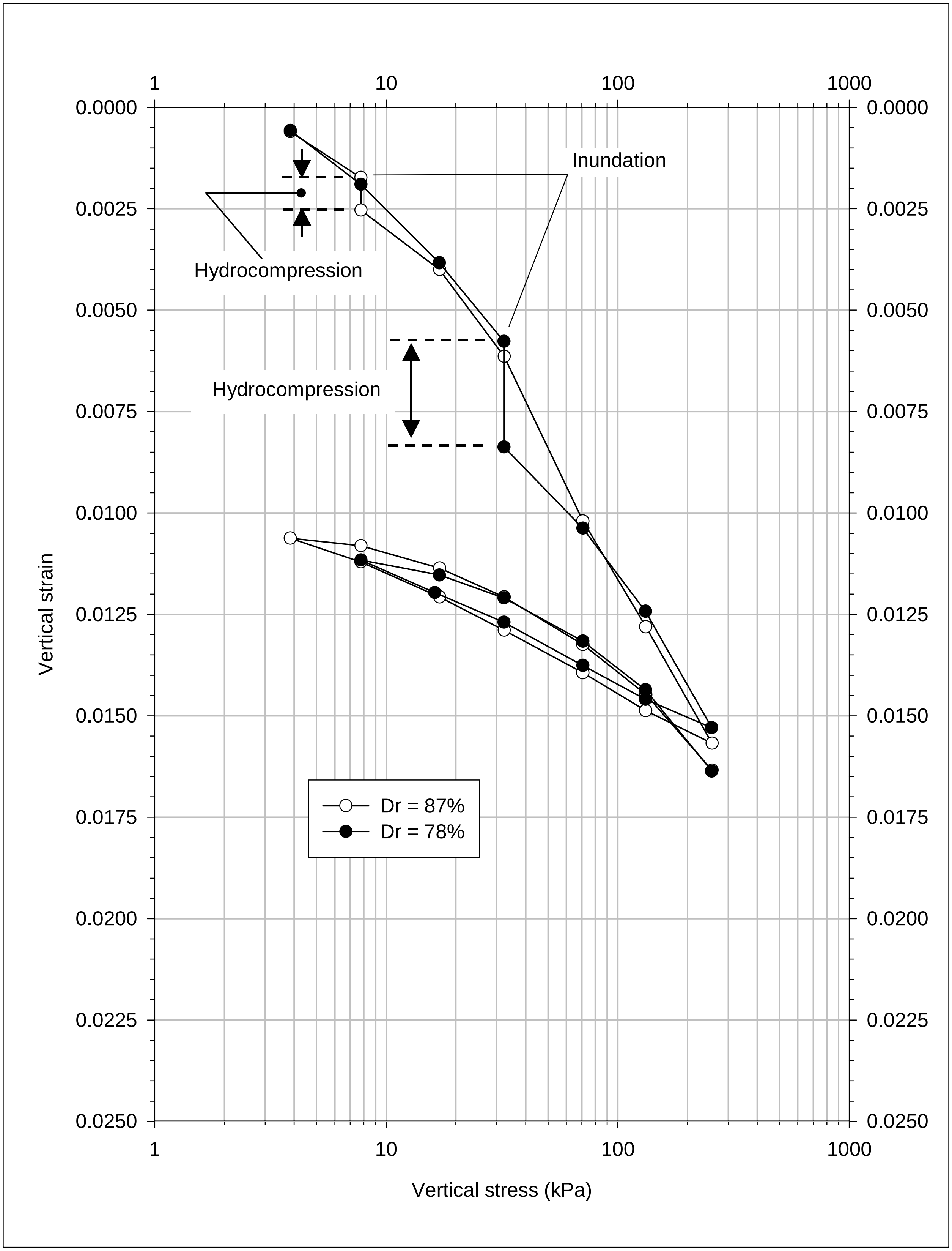

Figure A8. Results of consolidation tests on dense Light Castle Sand

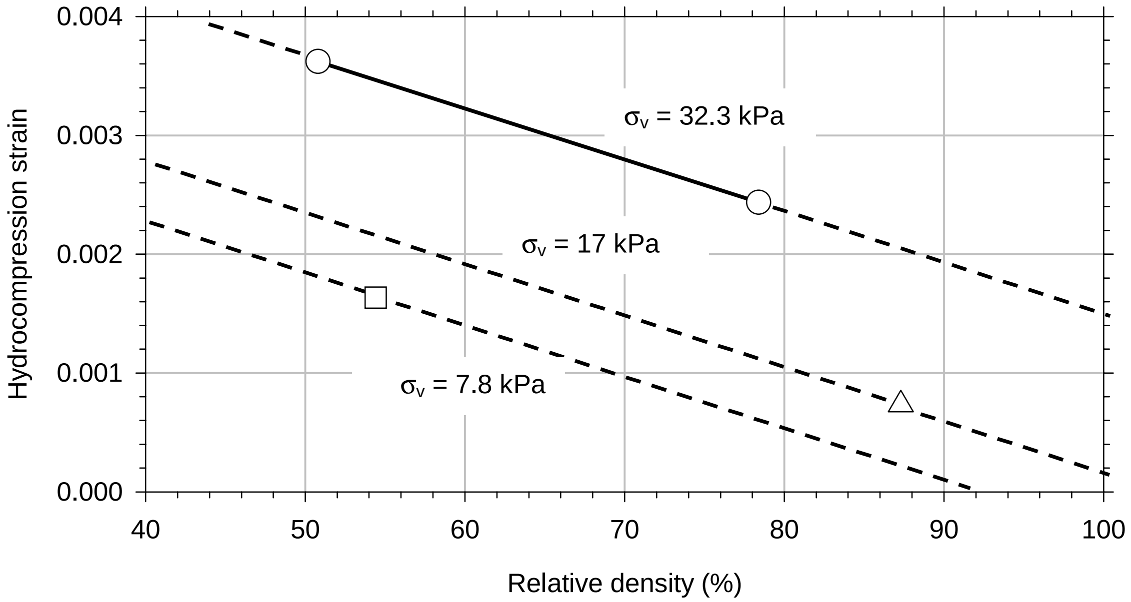

Figure A9. Relationship between hydrocompression strain and relative density for Light Castle Sand